

# Physical properties and doping characteristics of polyaniline–nylon 6 composite films

Sung Weon Byun<sup>a</sup> and Seung Soon Im<sup>b,\*</sup>

<sup>a</sup>*Korea Institute of Industrial Technology (KITECH), Textile and Cleaner Production, R&D Center, Chonan 330-820, Korea*

<sup>b</sup>*Department of Textile Engineering, College of Engineering, Hanyang University, Seoul 133-791, Korea*

(Received 31 July 1996; revised 20 January 1997)

Poly(aniline)–nylon 6 composite film (PANI-N) prepared by diffusion and chemical oxidative polymerization has very low percolation threshold contents (~4 wt%) and provides a high conductivity. Hydrogen bonding between poly(aniline) (PANI) and nylon 6 is found to affect the doping characteristics of PANI-N. From the results of dynamic mechanical thermal analysis, the crystalline regions of nylon 6 in the composites are found to be affected by the formation of PANI. From u.v.–visible spectra, it is considered that the thermal cross-linking reaction of PANI may be reversibly changed by the chemical doping and de-doping processes. © 1997 Elsevier Science Ltd.

(Keywords: poly(aniline); composites; percolation threshold)

## INTRODUCTION

An approach to improving the physical properties of electrically conductive poly(aniline) (PANI) is to form it into composite systems with common polymers that possess good mechanical properties, thus combining the desirable properties of both polymers<sup>1–5</sup>. It is important to minimize the content of PANI in composite systems to take advantage of the properties of the matrix polymer.

Recently, it has been reported that the hydrogen bonding between conducting polymers, e.g. poly(pyrrole) and poly(aniline), and host polymers, e.g. poly(vinyl alcohol) and poly(bisphenol A carbonate), can be formed in conductive polymer composite systems<sup>6,7</sup>. This hydrogen bonding between conductive polymer and host polymer is known to enhance the compatibility and physical properties of the composites. The interaction is considered to affect the physical properties and doping characteristics of the composites. However, little work has been done on these changes in the composites.

Previously, we have reported conductive polymer composite systems consisting of PANI and nylon 6 with the characteristic of transparency<sup>8,9</sup>. The conductivity and transmittance of these composite films were affected by the conditions of preparation. Moreover, we have recently studied the thermal stability of the conductivity of these composite systems, depending on the species of dopants with optical spectra<sup>10,11</sup>.

This paper reports the physical properties and doping characteristics of transparent and conductive poly(aniline)–nylon 6 composite systems which may contain hydrogen bonding between PANI and nylon 6, because this bonding can be considered to affect the doping characteristic of the conductive polymer composite. Therefore, in the presence of the interactions between conducting polymers and matrix polymers such as hydrogen bonding, the doping

characteristics of the conductive polymer in the composite system were studied in detail. The thermal and dynamic mechanical properties of the composite films were also studied systematically. After the undoped PANI composite films had been thermally treated, the structural changes in PANI due to protonic acid doping processes in the composite system were investigated by optical spectroscopy.

## EXPERIMENTAL

### *Preparation of poly(aniline)–nylon 6 composite films*

Transparent and conducting PANI–nylon 6 composite films (PANI-N) were prepared by immersing nylon 6 films (thickness 10  $\mu\text{m}$ , degree of crystallinity  $X_c = 21.0\%$ , Unitika Ltd) containing aniline monomer in an oxidant. This oxidant was aqueous ammonium peroxydisulfate solution containing one of various protonic acids such as hydrochloric acid, benzenesulfonic acid, sulfosalicylic and *p*-toluenesulfonic acid. Details of the procedure can be found in previous papers<sup>9,11</sup>. The as-prepared, doped PANI-N samples were converted to the de-doped forms by treatment with 0.5M aqueous KOH solution at room temperature for 2 h.

### *Determination of doping level of PANI-N*

The doping level of PANI-N was estimated from the contents of PANI and dopant anions in the composite films. First the as-prepared, doped PANI-N sample was thoroughly washed with distilled water and the extra dopant was removed from the surface of the composite film. The PANI content of the composite film was determined from the change in weight of the film before and after polymerization of PANI. The amount of dopant anions was determined by titration of chlorine or sulfur, using the combustion flask method<sup>12,13</sup>.

### *Characterization*

The conductivity of the composite films was measured

\*To whom correspondence should be addressed

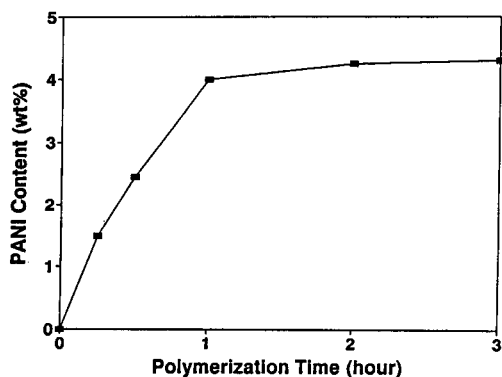


**Figure 1** Variation of PANI content with polymerization time in HCl-doped PANI-N. Polymerization temp. 4°C, oxidant conc. 0.25M, HCl conc. 1M

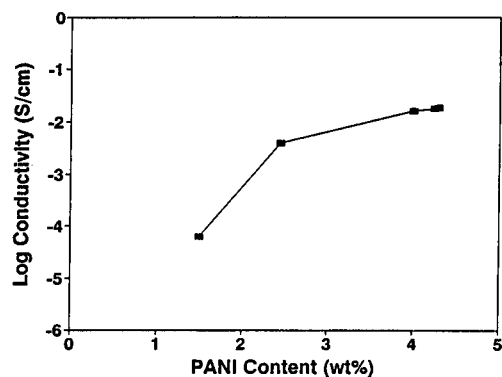


**Figure 2** Variation of conductivity with PANI content in HCl-doped PANI-N

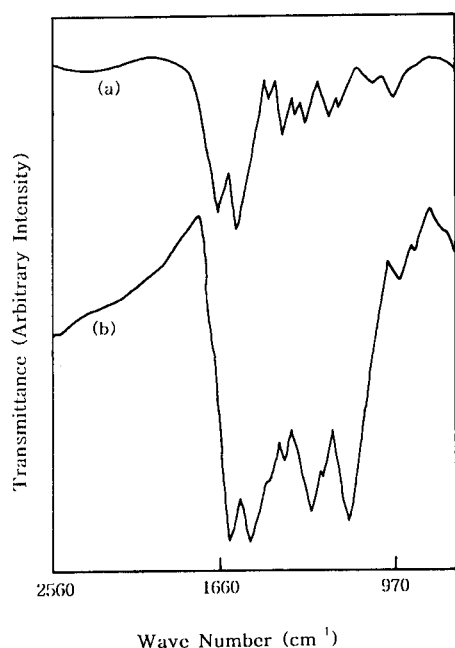


**Figure 3** FTIR spectra of (a) HCl-doped PANI powder and (b) HCl-doped PANI-N

Nicolet 5 DX system FTIR spectrometer, at a resolution of  $4\text{ cm}^{-1}$ . Differential scanning calorimetry (d.s.c.) was performed on a Du Pont 2100V 4.1C system at a heating rate of  $10^\circ\text{C min}^{-1}$  under a nitrogen atmosphere. Thermogravimetric analysis (t.g.a.) measurements were made using a Perkin-Elmer TGA 7 system under a nitrogen atmosphere with a programmed heating rate of  $10^\circ\text{C min}^{-1}$ . Dynamic mechanical thermal analysis (d.m.t.a., PL-DMTA MK III, Polymer Laboratories Ltd) was used to determine the storage modulus ( $E'$ ) and loss tangent ( $\tan \delta$ ) of PANI-N in the temperature range  $20\text{--}200^\circ\text{C}$ , with a heating rate of  $3^\circ\text{C min}^{-1}$  and a frequency of 5 Hz.

## RESULTS AND DISCUSSION

### Percolation threshold conductivity of PANI-N

The thickness of the as-prepared PANI-N was  $\sim 10\ \mu\text{m}$ . The sample film consisted of three layers<sup>9</sup>. The outer two layers were conducting composite layers and the inner layer was pristine nylon 6.

Figure 1 shows the effects of polymerization time on the content of HCl-doped PANI in the PANI-N. The PANI content of the composite films increased rapidly with polymerization time at first, but tended to level off after 1 h. In the first stage, it seems that PANI is mainly polymerized in the outer layer of the composite films and that this layer retards the diffusion of the oxidant solution to the interior side and prohibits PANI from being polymerized inside the film<sup>9</sup>. The absence of change after 1 h in the PANI content of the composite films can be explained by this phenomenon. It is difficult to control the PANI content because it is polymerized too rapidly.

Figure 2 shows the variation of conductivity with variation in HCl-doped PANI content for the composite films. The conductivity of PANI-N increases steeply as the PANI content increases, then reaches a maximum of  $\sim 3.5 \times 10^{-2}\ \text{S cm}^{-1}$  at  $\sim 4.4\ \text{wt}\%$ . The conductivity of pelletized PANI powder obtained by chemical synthesis under the same conditions was of the order of  $10^0\ \text{S cm}^{-1}$ . Generally, the upper limit of conductivity of the conductive composite materials prepared by mixing polymer matrices with conductive fillers such as carbon black, metal powders and conductive polymer powders can be achieved with a high weight fraction of the additives (usually  $> 20\ \text{wt}\%$ ). However, in our case the maximum conductivity of PANI-N could be reached at a very low PANI content ( $\sim 4\ \text{wt}\%$ ). It is noticeable that the PANI-N can show not only a lower percolation threshold but also a remarkably high conductivity. This means that the conductive paths of PANI in the PANI-N can be generated uniformly over the molecular chain gaps of the nylon 6 matrix film with a small amount of PANI.

### FTIR and u.v.–visible spectroscopy

The FTIR spectra of HCl-doped PANI and HCl-doped PANI-N are seen in Figure 3. For HCl-doped PANI, the characteristic absorption peaks are at 1589 and 1483 ( $\text{C}=\text{C}$  ring stretching), 1312 ( $\text{C}-\text{N}$  stretching) and  $1143\ \text{cm}^{-1}$  (vibrational mode of the imino-1,4-phenylene)<sup>15</sup>. The vibrational band characteristics of PANI at 1589, 1483, 1312 and  $1143\ \text{cm}^{-1}$  are shifted to 1575, 1465, 1301 and  $1135\ \text{cm}^{-1}$  respectively after formation of the composite film with nylon 6. A comparison of the spectrum of the PANI-N with the spectrum of PANI shows that the peak positions of PANI are shifted to lower wavenumbers. A

using the standard four-probe method<sup>14</sup>. The u.v.–visible absorption spectra of PANI-N were recorded on a UNICAM 8700 series spectrophotometer. FTIR analyses were made by the attenuated total reflectance (ATR) method on a

similar phenomenon was previously observed in other conductive polymer composite systems such as PANI–poly(vinyl alcohol) (PVA) and poly(pyrrole) (PPy)–PVA composites<sup>16,17</sup>. This indicates that hydrogen bonding is formed between PANI and nylon 6, which may result in weakening of bond strength in PANI.

Figure 4 shows the u.v.–visible spectra of the HCl-doped PANI-N and PANI coated on a quartz plate. For HCl-doped PANI, the absorption band at 345 nm is a  $\pi$ – $\pi^*$  transition and the absorbances at 400 and 815 nm arise from the polaron transitions<sup>18</sup>. These absorption bands for the PANI-N appear at 360, 420 and 840 nm respectively. This bathochromic shift (red shift) can also be considered to

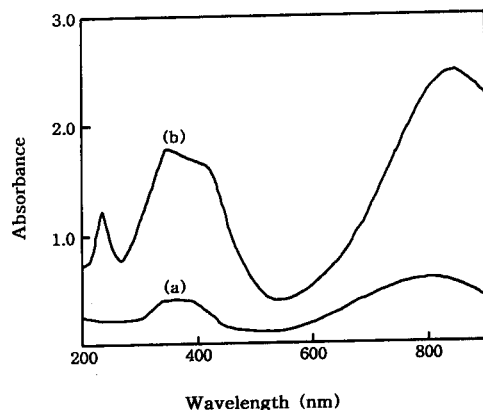


Figure 4 U.v.–visible spectra of (a) HCl-doped PANI powder and (b) HCl-doped PANI-N

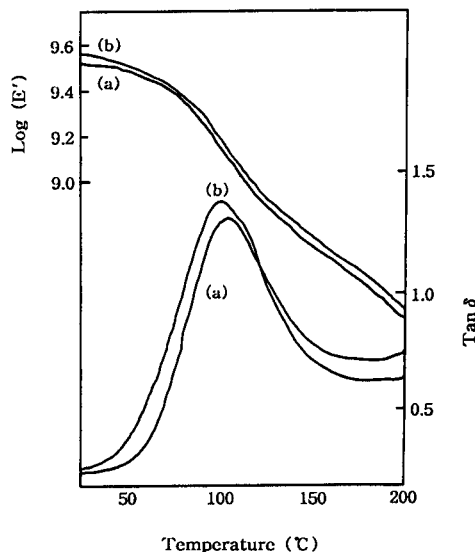


Figure 5  $\tan \delta$  and dynamic storage modulus as a function of temperature for (a) nylon 6 and (b) HCl-doped PANI-N

be due to the hydrogen bonding between nylon 6 and PANI. In the PANI-N, the absorption peak at 230 nm, which does not exist in pristine PANI, is due to aniline monomer remaining in the interior of the PANI-N<sup>11</sup>.

#### Doping characteristics of PANI-N

Table 1 shows the loadings of Cl or S in the PANI powder and PANI-N doped with various protonic acids, from which the doping level can be determined. Since the chemical formula of the fully doped PANI can be represented approximately by  $[(C_{24}H_{18}N_4) \cdot 2HA]_m$ , the theoretical amount of Cl and S can be roughly calculated from this formula. The amount of Cl in the HCl-doped PANI powder prepared is 2.27 wt% and the ratio to the theoretical value (2.47 wt%) is 91.9%. In the case of HCl-doped PANI-N, the weight ratio of PANI to nylon 6 in the composite film is 4.4%, and the measured amount of Cl is 1.57 wt%. The Cl loading of HCl-doped PANI-N as a proportion of that of the HCl-doped PANI powder ( $V_p/V_c$ ) is  $\sim 69\%$ . Thus the HCl-doped PANI-N has a lower doping level than that of PANI powder prepared under the same conditions. This phenomenon is also observed for PANI-N doped with other protonic acids (Table 1). It seems that this result is due to the hydrogen bonding between PANI and nylon 6<sup>17</sup>. It is considered that the hydrogen bonding may result in weakening of the doping ability of PANI in the composite.

#### D.m.t.a. of PANI-N

Dynamic mechanical thermal analysis (d.m.t.a.) curves for nylon 6 and HCl-doped PANI-N are given in Figure 5. For nylon 6,  $\tan \delta$  shows  $T_g$  to lie at 105°C. It is higher than that normally observed, 70°C, because the film is biaxially stretched and its degree of crystallinity is as high as 21%. For HCl-doped PANI-N, the  $\tan \delta$  curve shows the presence of  $T_g$  at 97°C (Figure 5b). This  $\tan \delta$  peak is slightly broader than that of the nylon 6 and its intensity is increased. This indicates that nylon 6 domains are affected by the PANI in the composite. This can be attributed to the hydrogen bonding interaction at the boundaries between PANI and the nylon 6 phases, and the deformation of nylon 6 crystal structure through the formation of PANI in the composite film. The intensity of the  $\tan \delta$  peak is often given by the following equation<sup>19</sup>:

$$\tan \delta = X_c(\tan \delta)_c + (1 - X_c)(\tan \delta)_a \quad (1)$$

where  $X_c$  is the degree of crystallinity, and the subscripts a and c refer to the contributions of the amorphous and pure crystalline phases respectively. In general, since  $\tan \delta$  is mostly due to the amorphous phase, equation (1) simplifies to the following equation:

$$\tan \delta = (1 - X_c)(\tan \delta)_a \quad (2)$$

This equation shows that the intensity of  $\tan \delta$  decreases with increasing degree of crystallinity.

Table 1 Variation of Cl and S loadings in PANI powder and PANI-N doped with various protonic acids

	Loading of Cl or S (wt%)				
	Theoretical value, $V_t$	Experimental value for PANI powder, $V_p$	Experimental value for PANI-N, $V_c$	$100V_p/V_t$	$100V_c/V_t$
HCl-doped PANI-N (4.4 wt%)	2.47	2.27	1.57	91.9	63.6
BSA-doped PANI-N (4.0 wt%)	9.32	8.57	6.24	92.0	70.0
SSA-doped PANI-N (4.2 wt%)	12.86	11.56	8.35	89.9	64.9
TSA-doped PANI-N (3.7 wt%)	8.58	7.72	5.84	90.0	68.1

**Table 2** Heat of fusion, melting temperature and degree of crystallinity of nylon 6 and HCl-doped PANI-N

	Heat of fusion, $\Delta H_f$ ( $J g^{-1}$ )	Melting point, $T_m$ ( $^{\circ}C$ )	Degree of crystallinity, $X_c$ (%)
Nylon 6	55.28	217.4	21.0
HCl-doped PANI-N	49.40	215.5	18.7

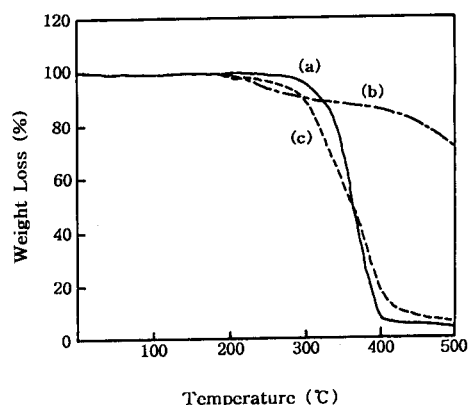
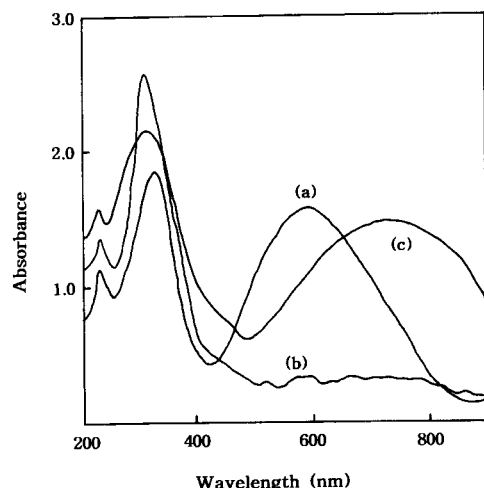
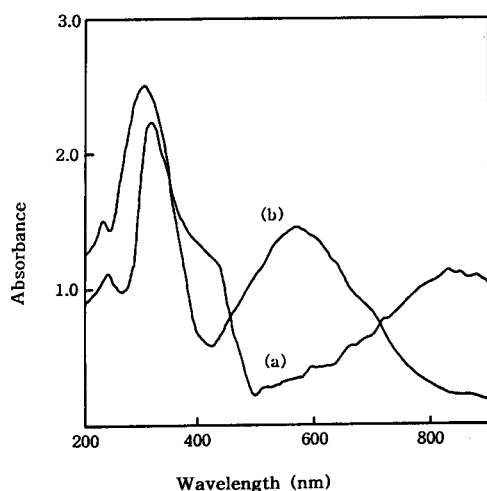

**Figure 6** T.g.a. curves of (a) nylon 6, (b) HCl-doped PANI powder and (c) HCl-doped PANI-N

**Figure 7** U.v.-visible spectra of (a) undoped PANI-N, (b) thermally treated PANI-N and (c) thermally treated HCl-doped PANI-N. Thermal treatment at  $180^{\circ}C$  for 1 h

**Figure 8** U.v.-visible spectra of (a) HCl-doped PANI-N and (b) de-doped PANI-N in 0.5M aqueous KOH after thermal treatment at  $180^{\circ}C$  for 1 h

Table 2 shows the degree of crystallinity of nylon 6 and HCl-doped PANI-N. As can be seen, the degree of crystallinity of PANI-N is somewhat reduced and the melting point shifts to a slightly lower temperature compared with nylon 6. This means that the crystalline regions are partly destroyed by the formation of PANI in the composite. This result is in good agreement with that of d.m.t.a. Therefore the increase in the  $\tan \delta$  peak intensity in PANI-N can be explained by the decrease in the crystallinity of nylon 6 (equation (2)).

Figure 6 shows the thermogravimetric analysis (t.g.a.) curves of the nylon 6, HCl-doped PANI and HCl-doped PANI-N. The HCl-doped PANI shows a two-step decomposition. The first weight loss begins at  $180^{\circ}C$  and continues up to  $300^{\circ}C$ ; the weight loss is  $\sim 10\%$ , corresponding to the weight loss of the counter-anions. The second step starting at  $420^{\circ}C$  corresponds to the decomposition of the backbone structure<sup>20</sup>. Nylon 6 shows only one major weight loss at  $\sim 320^{\circ}C$ , attributed to structural decomposition. The PANI-N exhibits a lower decomposition temperature than that of nylon 6, but the slope of the decomposition curve is more gentle. The t.g.a. curve of the PANI-N does not show the significant improvement in thermal stability which has been reported for other conductive polymer composite systems<sup>6,7</sup>.

#### Structural changes in undoped PANI-N

The HCl-doped PANI-N was converted to the undoped form (base form) in 0.5M aqueous KOH and the undoped PANI-N was treated at  $180^{\circ}C$  for 1 h. Figure 7 shows the u.v.-visible spectra of the undoped and thermally treated PANI-N. In the undoped PANI-N (Figure 7a), the absorption bands at  $\sim 323$  and 590 nm represent the  $\pi-\pi^*$  transition and the excitation band of the quinoid ring respectively<sup>18</sup>. On thermal treatment of this composite film (Figure 7b), the excitation band of the quinoid ring disappears. This change is considered to be due to the thermal cross-linking of the PANI, which has been suggested to occur between the quinoid ring and imine group<sup>21</sup>. In the case of HCl-doped PANI-N, the three-band spectrum (Figure 4b) is changed to a two-band spectrum which is found in the undoped form of PANI-N after thermal treatment (Figure 7c). Concurrent with this change is a dramatic drop in the electrical conductivity of the PANI-N. On re-doping of thermally treated PANI-N with HCl (Figure 8a), the absorption bands appear at 420 and 840 nm which are due to the polaron band transitions. And when this re-doped PANI-N is de-doped in 0.5M KOH solution for 2 h, the excitation band of the quinoid ring appears again at 590 nm (Figure 8b). Although the spectra are not shown in this paper, this phenomenon was also observed in the PANI treated with various other protonic acids such as benzenesulfonic acid, sulfosalicylic acid and *p*-toluenesulfonic acid. This is a very interesting phenomenon. It means that the thermally cross-linked PANI can be doped with protonic acids and the thermal cross-linking reaction of PANI may be reversibly changed by protonic acid doping and chemical de-doping processes.

## CONCLUSIONS

It has been shown that PANI-N prepared by diffusion and chemical oxidative polymerization can present not only a lower percolation threshold but also a remarkably high conductivity. Hydrogen bonding between PANI and nylon 6 has been identified by FTi.r. and u.v.-visible spectroscopy, and may result in a weakening of the doping ability of PANI. The d.m.t.a. results indicate that the crystalline regions of nylon 6 in the composite film are partly destroyed by the formation of PANI. It has been found that the thermal cross-linking reaction of PANI may be reversibly changed by the chemical doping and de-doping processes. Further work is in progress to clarify the nature of this reversible thermal cross-linking reaction of PANI through chemical doping.

## ACKNOWLEDGEMENTS

This work was carried out under research promotion grants from the Korea Research Foundation and a research grant from the Korea Science and Engineering Foundation (9223-0006).

## REFERENCES

1. Pei, Q. and Bi, X., *J. Appl. Polym. Sci.*, 1989, **38**, 1819.

2. Andreatta, A., Heerger, A. J. and Smith, P., *Polym. Commun.*, 1990, **31**, 275.
3. Xue, Z. and Bi, X., *J. Appl. Polym. Sci.*, 1993, **47**, 2073.
4. Yang, S. and Ruckenstein, E., *Synth. Met.*, 1993, **59**, 1.
5. Morita, M. and Hashida, I., *J. Appl. Polym. Sci.*, 1990, **41**, 1073.
6. Wang, H. L., Toppare, L. and Fernandez, J. E., *Macromolecules*, 1990, **23**, 1053.
7. Wang, H. L. and Fernandez, J. E., *Macromolecules*, 1992, **25**, 6179.
8. Byun, S. W. and Im, S. S., *Synth. Met.*, 1993, **57**, 3501.
9. Byun, S. W. and Im, S. S., *J. Appl. Polym. Sci.*, 1994, **51**, 1221.
10. Byun, S. W. and Im, S. S., *Synth. Met.*, 1995, **69**, 219.
11. Byun, S. W. and Im, S. S., *J. Appl. Polym. Sci.*, 1995, **56**, 425.
12. Belcher, R., *Instrumental Organic Elemental Analysis*. Academic Press, New York, 1977.
13. Ma, T. S. and Rittner, R. C., *Modern Organic Elemental Analysis*. Dekker, New York, 1979.
14. Runyan, W. R., *Semiconductor Measurements and Instrumentation*. McGraw-Hill, New York, 1975.
15. Tang, J., Jing, X., Wang, B. and Wang, F., *Synth. Met.*, 1988, **24**, 231.
16. Chen, S. A. and Fang, W. G., *Macromolecules*, 1991, **24**, 1242.
17. Wang, H. L. and Fernandez, J. E., *Macromolecules*, 1993, **26**, 3336.
18. Wan, M., *Synth. Met.*, 1989, **31**, 51.
19. Gray, R. W. and McCrum, N. G., *J. Polym. Sci. A2*, 1969, **7**, 1329.
20. Wei, Y. and Hsueh, K. F., *J. Polym. Sci. A, Polym. Chem.*, 1989, **27**, 4351.
21. MacDiarmid, A. G., Scherr, E. M., Manohar, S. K., Masters, T. G., Sun, Y., Tang, X., Druy, M. A., Glatkowski, P. J., Cajipe, V. B., Fisher, J. E., Cromack, K. R., Jozefowicz, M. E., Ginder, J. M., MacCall, R. P. and Epstein, A. J., *Synth. Met.*, 1991, **43**, 735.